PROCEEDINGS OF SPIE

SPIEDigitalLibrary.org/conference-proceedings-of-spie

Wide field-of-view waveguide displays enabled by polarization-dependent metagratings

Zhujun Shi, Wei Ting Chen, Federico Capasso

Zhujun Shi, Wei Ting Chen, Federico Capasso, "Wide field-of-view waveguide displays enabled by polarization-dependent metagratings," Proc. SPIE 10676, Digital Optics for Immersive Displays, 1067615 (21 May 2018); doi: 10.1117/12.2315635

SPIE.

Event: SPIE Photonics Europe, 2018, Strasbourg, France

Downloaded From: https://www.spiedigitallibrary.org/conference-proceedings-of-spie on 1/23/2019 Terms of Use: https://www.spiedigitallibrary.org/terms-of-use

Wide field-of-view waveguide displays enabled by polarization-dependent metagratings

Zhujun Shi[a], Wei Ting Chen[b], Federico Capasso[b*]

[a]Department of Physics, Harvard University, Cambridge, MA, USA 02138; [b]John A. Paulson School of Engineering and Applied Sciences, Harvard University, Cambridge, MA, USA 02138
*Corresponding author: capasso@seas.harvard.edu

ABSTRACT

We proposed a waveguide display design based on polarization dependent metagratings. By encoding the left and right half of field of view (FOV) in two orthogonal polarization channels, we achieved an overall horizontal FOV of 67° at 460 nm using a single waveguide, which is 70% larger than that achieved with conventional diffractive gratings. Metagratings that selectively diffract out TE or TM polarized light are designed and simulated using rigorous coupled wave analysis (RCWA). High polarization selectivity is achieved, with minimal crosstalk between the two channels. The transmission spectrum at normal incidence is calculated to assess the see-through effect. Remaining challenges such as fabrication and efficiency issues are discussed. The concept of multiplexing information in the polarization domain enables wide FOV waveguide displays for future AR devices.

Keywords: Waveguide display, polarization multiplexing, metasurface, field of view

1. INTRODUCTION

With the broad range of potential applications in healthcare, education, gaming, navigation and advertising, augmented reality (AR) technology has gained great attention in recent years. By bringing together the virtual images and the real world into a person's perception, AR devices provide an immersive and enriched experience to the viewers. One key hardware component of AR devices is the see-through optical combiner, which combines and delivers the virtual image and real world optically in front of the eyes.

Several types of optical combiner architecture have been proposed, using either refractive/reflective, diffractive, holographic optics, or a combination of them[1]. Examples of refractive/reflective optics based designs include 50/50 beam splitters placed at 45° in front of the viewers and total internal reflection (TIR) prism lenses using freeform surfaces. Although conceptually intuitive, these devices are usually heavy and bulky. Holographic optical waveguide technology enables light-weight, relatively thin planar optical combiners with large eyeboxes[2]. In this approach, a volume hologram, either in transmission or reflection mode, is used to progressively extract the light guided by TIR in the planar glass plate. The spectral and angular selectivity is designed to achieve larger field of view (FOV) and operation with broader spectral sources. One major drawback of this approach is the sensitivity of volume holographic media. The material used in the volume holograms limits the device lifetime, especially when exposed to harsh environment. Another typical optical combiner architecture uses diffractive gratings, such as surface relief gratings, instead of volume holograms[3, 4]. This architecture allows for easier mass manufacturing, relatively high efficiency and a good trade-off between the spectral/angular bandwidth requirements. To realize a full-color display, usually three layers of waveguide gratings corresponding to red, green and blue (RGB) light are stacked together. Each layer is designed to extract light at a specific spectral range. Other optical combiner architectures like arrayed reflectors have also been patented and demonstrated.

In this paper, we focus on the diffractive grating based optical combiner architecture. Despite the various implementations, the FOV in the diffractive grating based approaches is ultimately limited by the waveguide refractive index. Typically, for a waveguide refractive index of 1.7, the maximum achievable horizontal FOV is less than 40°. Here, we break away from this limit and achieve a horizontal FOV as large as 67° using polarization dependent metagratings. Similar to polarization division multiplexing in optical fiber communications where two channels with orthogonal polarizations are used to double the information capacity, here we increase the FOV by encoding the left and right FOV into two orthogonal polarization channels, TE and TM, respectively. Polarization dependent metagratings, which consist of subwavelength patterned nanosctructures, are designed to selectively extract TE or TM light only (TE-pass grating and TM-pass grating). The out-

Digital Optics for Immersive Displays, edited by Bernard C. Kress, Wolfgang Osten, Hagen Stolle, Proc. of SPIE Vol. 10676, 1067615 · © 2018 SPIE
CCC code: 0277-786X/18/$18 · doi: 10.1117/12.2315635

Downloaded From: https://www.spiedigitallibrary.org/conference-proceedings-of-spie on 1/23/2019
Terms of Use: https://www.spiedigitallibrary.org/terms-of-use

coupler consists of alternate columns of TE-pass and TM-pass gratings. As a proof-of-principle demonstration, here we only consider 1D eyebox expansion (horizontal FOV) at a single wavelength. The design approach can be generalized to full-color 2D eyebox expansion by introducing additional diffractive optical elements that redirect the guided light at 90° and stacking three layers (RGB) of waveguides together.

2. WORKING PRINCIPLE

Figure 1(a) illustrates the schematic of the polarization dependent metagrating based optical combiner. Linear polarizers that transmit x (TM) polarization or y (TE) polarization are placed in front of the right or left part of the microdisplay panel respectively. After passing through the collimator, light from the left (TE) or right (TM) part of the FOV interacts with the in-coupler and becomes guided by TIR in the waveguide. The grating couplers are designed to impart different transverse momentum to TE and TM light selectively, such that light from both the left and right half of the FOV becomes guided by TIR. When reaching the polarization dependent metagrating out-coupler, TE and TM light is diffracted to the right and left respectively, recovering the displayed image.

The polarization selectivity is achieved by spatially interleaving two types of metagratings, TE-pass and TM-pass gratings (Fig. 1(b)). The two types of metagratings have different grating periods, therefore TE and TM light from the same incident angle is diffracted to different output angles. To avoid crosstalk, the metagratings are designed to diffract out only light of a particular polarization, and reflect back the other polarization (Fig. 1(b)).

In conventional waveguide gratings, there is a one-on-one correspondence between the guided angle in the waveguide and output diffraction angle. In our method, however, a specific guided angle is mapped to two different output angles. This is the key working principle of our design.

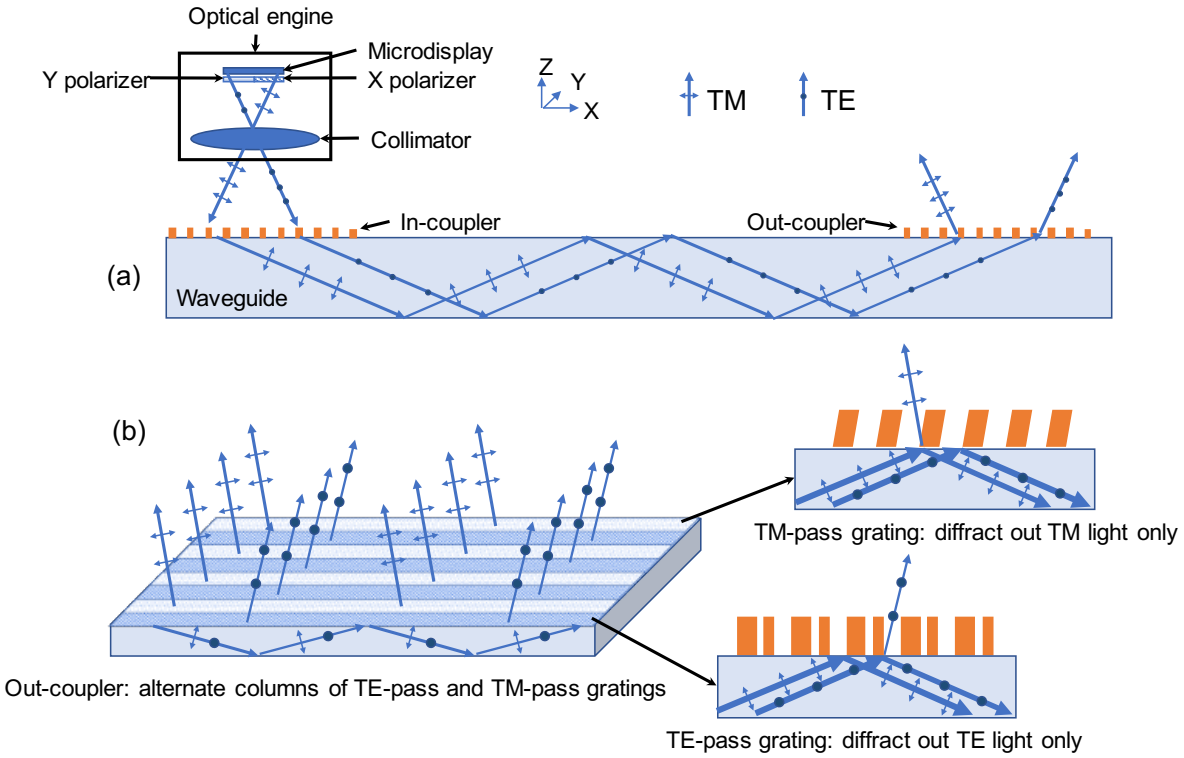

Figure 1. (a) Schematic of the polarization dependent metagrating based design. The optical engine consists of a microdisplay, two orthogonal linear polarizers covering the left and right half of the display respectively, and a collimator. The in-coupler and out-coupler are responsible for coupling in and out the free space light to guided light. The waveguide is a high-index glass plate. (b) Schematic of the out-coupler. TE-pass and TM-pass gratings are spatially multiplexed together. The zoom-in view shows that the two types of metagratings are patterned with different nanostructures and have different grating periods. The TE (TM) -pass grating diffracts out TE (TM) light only, and reflects the TM (TE) light.

Downloaded From: https://www.spiedigitallibrary.org/conference-proceedings-of-spie on 1/23/2019
Terms of Use: https://www.spiedigitallibrary.org/terms-of-use

3. THEORY

Figure 2(a) illustrates the achievable horizontal FOV in a conventional diffractive grating out-coupler. The light guided in the waveguide is constrained within a cone $\theta_{inc,min} \sim \theta_{inc,max}$. To satisfy the TIR condition, $\theta_{inc,min}$ is required to be no smaller than $\theta_{TIR} = \text{asin}\frac{1}{n}$, where n is the refractive index of the glass plate (n =1.7 in the following calculation). The maximum allowable angle $\theta_{inc,max}$ is determined by the device geometry. In our design, we assume $\theta_{inc,max}$=75°. For a given grating period P, the output angle is given by the grating equation

$$n \sin\theta_{inc} - \frac{\lambda}{P} = \sin\theta_{out} \tag{1}$$

If $\theta_{out,min} = -\theta_{out,max}$, then the maximum FOV and the corresponding grating period P are given by

$$\text{FOV}_{max} = \theta_{out,max} - \theta_{out,min} = 2\text{asin}\left(\frac{n\sin 75° - 1}{2}\right) = 37.5° \tag{2}$$

$$\text{P} = \frac{2\lambda}{n\sin 75° + 1} = 0.76\lambda \tag{3}$$

It can be proved that for general cases where $\theta_{out,min} \neq -\theta_{out,max}$, the maximum achievable FOV is less than 40° as long as the center of the FOV, $(\theta_{out,min} + \theta_{out,max})/2$, is less than 15° away from the normal direction.

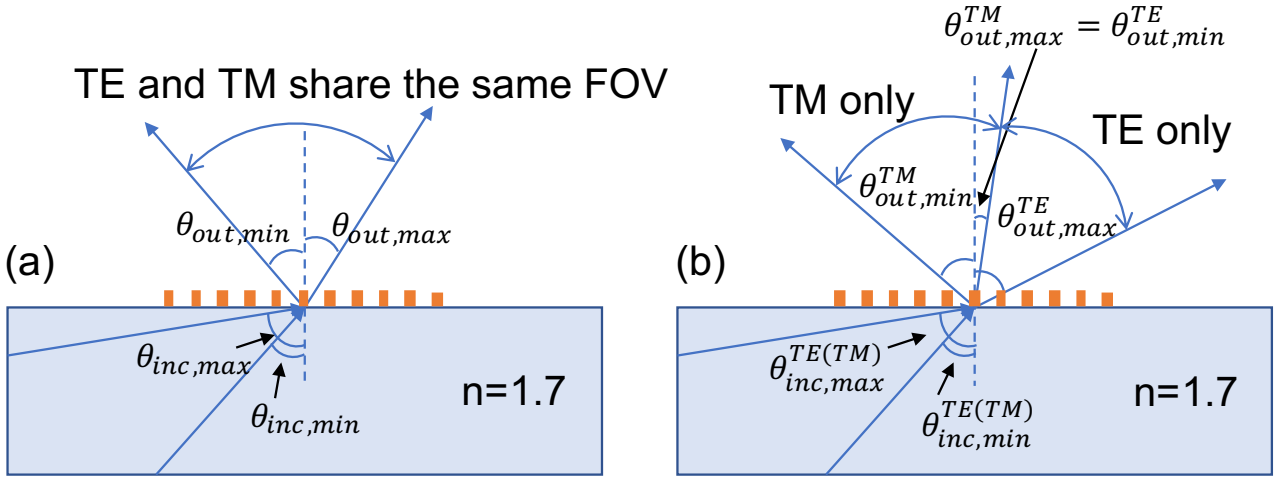

Figure 2. (a) Conventional diffractive grating out-coupler. TE and TM light share the same FOV. (b) Polarization dependent metagrating based out-coupler. TE and TM light is diffracted to two separate viewing zones. The overall FOV is greatly increased.

In our design (Fig. 2(b)), the out-coupler imparts a different transverse momentum to TE and TM light. The grating period of the TE-pass and TM-pass grating is denoted by P_{TE} and P_{TM} respectively. Here P_{TE} is larger than P_{TM} so that TE and TM light is diffracted to the right and left region respectively. The grating equations become

$$n \sin\theta^{TE}_{inc} - \frac{\lambda}{P_{TE}} = \sin\theta^{TE}_{out} \tag{4}$$

$$n \sin\theta^{TM}_{inc} - \frac{\lambda}{P_{TM}} = \sin\theta^{TM}_{out} \tag{5}$$

To avoid any gap or overlap in the FOV, it is required that

$$\theta^{TM}_{out,max} = \theta^{TE}_{out,min} \tag{6}$$

As a proof-of-principle demonstration, we designed the metagratings for blue light, $\lambda = 460\ nm$. The grating periods are chosen to satisfy the constraints mentioned above, $P_{TE} = 460\ nm, P_{TM} = 315\ nm$. In addition, we have $\theta^{TM}_{inc,max} = \theta^{TE}_{inc,max} = 75°$, $\theta^{TM}_{inc,min} = \text{asin}\frac{1}{n} = 37°, \theta^{TE}_{inc,min} = 44°$.

Downloaded From: https://www.spiedigitallibrary.org/conference-proceedings-of-spie on 1/23/2019
Terms of Use: https://www.spiedigitallibrary.org/terms-of-use

Plugging the parameters into Eqn. (4)-(6), we get $\theta_{out,min}^{TM} = -27°, \theta_{out,max}^{TE} = 40°, \theta_{out,max}^{TM} = \theta_{out,min}^{TE} = 10.4°$. The achieved total horizontal FOV is

$$\text{FOV} = \theta_{out,max}^{TE} - \theta_{out,min}^{TM} = 67°$$

Which is around 70% larger than the maximum horizontal FOV achieved in conventional diffractive grating designs.

4. RESULTS

The schematic of the metagrating unit cells is shown in Fig. 3(a)-(b). The TM-pass grating is slanted at 40° to increase the TM light out-coupling efficiency at large incident angles. The TE-pass grating consists of two rectangular ridges within each unit cell. It is important to mention here that the two metagratings have different slanted angle, height and refractive indices, which poses significant fabrication challenges. For future works, more advanced optimization methods (e.g. topological optimization)[5] may be used to realize TE- and TM-pass metagratings that have the same refractive index, height and slanted angle.

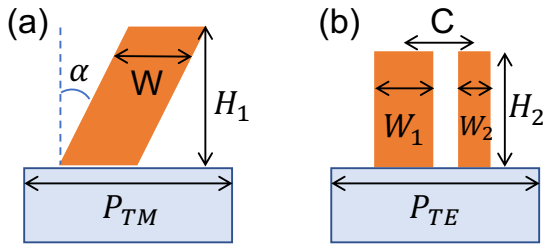

Figure 3. (a) Unit cell of a TM-pass grating. The slanted ridge has a refractive index of 2.4. $H_1 = 350\ nm$, $W = 280\ nm$. The slanted angle is $\alpha = 40°$. The unit cell size (grating period) is $P_{TM} = 315\ nm$. (b) Unit cell of a TE-pass grating. The rectangular ridges have a refractive index of 1.716. $H_2 = 250\ nm$, $W_1 = 90\ nm$, $W_2 = 40\ nm$. The center to center distance is $C = 140\ nm$. The unit cell size (grating period) is $P_{TE} = 460\ nm$.

We calculated the grating diffraction efficiency for TE and TM light into each order using rigorous coupled wave analysis (RCWA) [6]. The transmitted -1st is the desired out-coupling order. The reflected 0th order carries the guided light to propagate down the waveguide. All other diffraction orders are deemed unwanted. Figure 4(a)-(b) shows the diffraction efficiency as a function of the incident angles. One can see that the transmitted -1st order of TM (TE) light is negligible in TE (TM) pass gratings, in accordance with the required polarization selectivity. There are some remaining unwanted orders, which causes efficiency loss and need to be improved in future designs. Although a source of loss, however, the unwanted orders do not necessarily introduce ghost images, as they are mostly reflected at an angle smaller than TIR and will leave the waveguide at the backside (the environment side).

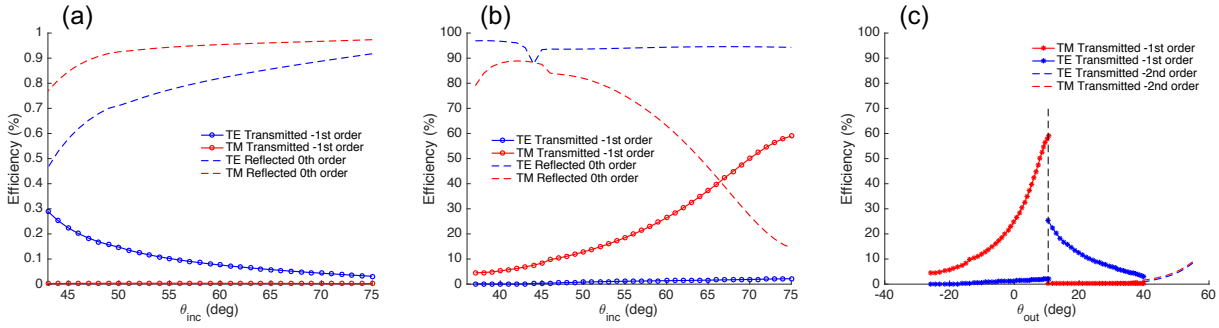

Figure 4. (a) Diffraction efficiency of TE-pass gratings as a function of incident angles (guided angles inside the waveguide). (b) Diffraction efficiency of TM-pass gratings as a function of incident angles (guided angles inside the waveguide). (c) Overall diffraction efficiency in the transmission (including both TE and TM pass gratings) as a function of the output angles.

Downloaded From: https://www.spiedigitallibrary.org/conference-proceedings-of-spie on 1/23/2019
Terms of Use: https://www.spiedigitallibrary.org/terms-of-use

Figure 4(c) shows the diffraction efficiency of the transmitted orders as a function of the output angles. One can see that the left (right) half of FOV contains TM (TE) light only. There is some residue unwanted higher order (transmitted -2nd order), but it falls outside of the FOV and does not interfere with the virtual image.

In addition to the FOV of virtual images, see-through effect is another critical performance criterion for optical combiners. It is required that the real world image is minimally altered, ideally unaltered, after passing through the optical combiner. We characterize the see-through performance of the metagratings by their transmission efficiency under normal incidence (Fig. 5). The overall transmission, averaged over TE and TM light, is relatively flat across the visible spectrum, with a mean transmission efficiency of 75%.

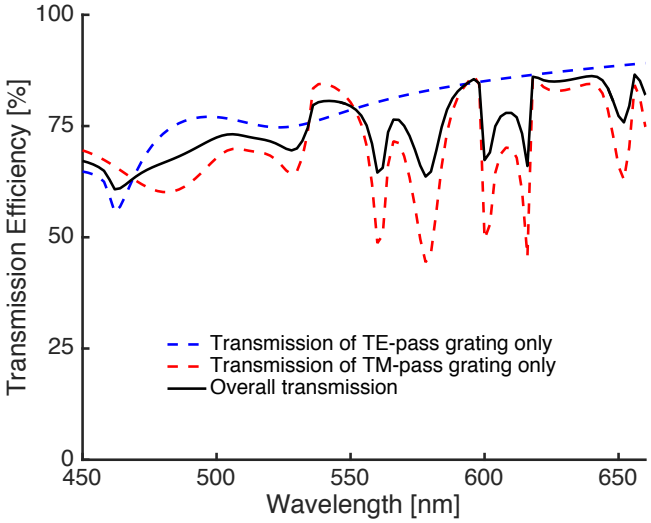

Figure 5. Transmission efficiency at normal incidence. Blue dashed line: transmission spectrum of TE-pass gratings; red dashed line: transmission spectrum of TM-pass gratings; black solid line: overall transmission, averaged over TE and TM pass gratings.

5. SUMMARY AND DISCUSSION

We proposed a waveguide display design based on polarization dependent metagratings. By encoding the left and right half of FOV in orthogonal polarization channels, we increased the horizontal FOV by 70%, compared to designs based on conventional diffractive gratings. Metagratings that selectively diffract out TE or TM polarized light are designed and simulated. High polarization selectivity is achieved, with minimal crosstalk between the two channels. There are several remaining challenges that need to be addressed in future designs. First, the TE and TM pass gratings used in this paper must be fabricated separately. In the future, more advanced optimization tools may be utilized to achieve unit cell designs with the same material, height and slanted angle for both TE and TM pass gratings, so that they can be fabricated in a single step. Second, the residue unwanted orders introduce loss of efficiency, and need to be further suppressed. Third, there is a large variation of diffraction efficiency across the FOV. For best use of the display's dynamic range and viewing experience, it is desired to have a more uniform diffraction efficiency. Despite of the remaining challenges, we believe that the concept of multiplexing information in the polarization domain is important for achieving larger FOV in future AR devices.

ACKNOWLEDGEMENT

This research is supported by in part by the Air Force Office of Scientific Research (MURI FA9550-14-1-0389 and FA9550-16-1-0156). Z.S. thanks Zhehao Dai and Joon-Suh Park for helpful discussion.

Downloaded From: https://www.spiedigitallibrary.org/conference-proceedings-of-spie on 1/23/2019
Terms of Use: https://www.spiedigitallibrary.org/terms-of-use

REFERENCES

[1] B. Kress, and T. Starner, "A review of head-mounted displays (HMD) technologies and applications for consumer electronics," Photonic Applications for Aerospace, Commercial, and Harsh Environments Iv, 8720, (2013).

[2] H. Mukawa, K. Akutsu, I. Matsumura *et al.*, "A full-color eyewear display using planar waveguides with reflection volume holograms," Journal of the Society for Information Display, 17(3), 185-193 (2009).

[3] T. Levola, "Diffractive optics for virtual reality displays," Journal of the Society for Information Display, 14(5), 467-475 (2006).

[4] T. Levola, and P. Laakkonen, "Replicated slanted gratings with a high refractive index material for in and outcoupling of light," Optics Express, 15(5), 2067-2074 (2007).

[5] D. Sell, J. J. Yang, S. Doshay *et al.*, "Large-Angle, Multifunctional Metagratings Based on Freeform Multimode Geometries," Nano Letters, 17(6), 3752-3757 (2017).

[6] J. P. Hugonin and P. Lalanne, RETICOLO code for grating analysis, Palaiseau, France: Institute d'Optique, 2005.

Downloaded From: https://www.spiedigitallibrary.org/conference-proceedings-of-spie on 1/23/2019
Terms of Use: https://www.spiedigitallibrary.org/terms-of-use